Electronic Supplementary Material (ESI) for Journal of Materials Chemistry A.

Supplementary Information

Systematic comparison of different dopants in thin film hematite (α-Fe_2O_3) photoanodes for solar water splitting

Kirtiman Deo Malviya, Hen Dotan, Dmitry Shlenkevich, Anton Tsyganok, Hadar Mor, Avner Rothschild*

Department of Materials Science and Engineering, Technion - Israel Institute of Technology, Haifa, Israel.

Corresponding author: Avner Rothschild

Email: avner@mt.technion.ac.il

Table S1. The relative density and chemical composition of all the targets, and the composition of two thick (~1 μm) films deposited from the Nb and Ti-doped Fe_2O_3 targets.

Dopant	Density of the target (%)	Dopant concentration in the target (cation%)	Dopant concentration in the film (cation%)
TiO_2	88	1.3 ± 0.2	0.8 ± 0.2
Nb_2O_5	88	1.3 ± 0.1	1.3 ± 0.2
SnO_2	92	1.2 ± 0.1	
ZrO_2	93	1.3 ± 0.2	
PtO_2	85	0.81 ± 0.02	
SiO_2	93	0.43 ± 0.03	
ZnO	94	0.89 ± 0.04	
NiO	91	0.9 ± 0.2	
MnO	90	1.1 ± 0.1	

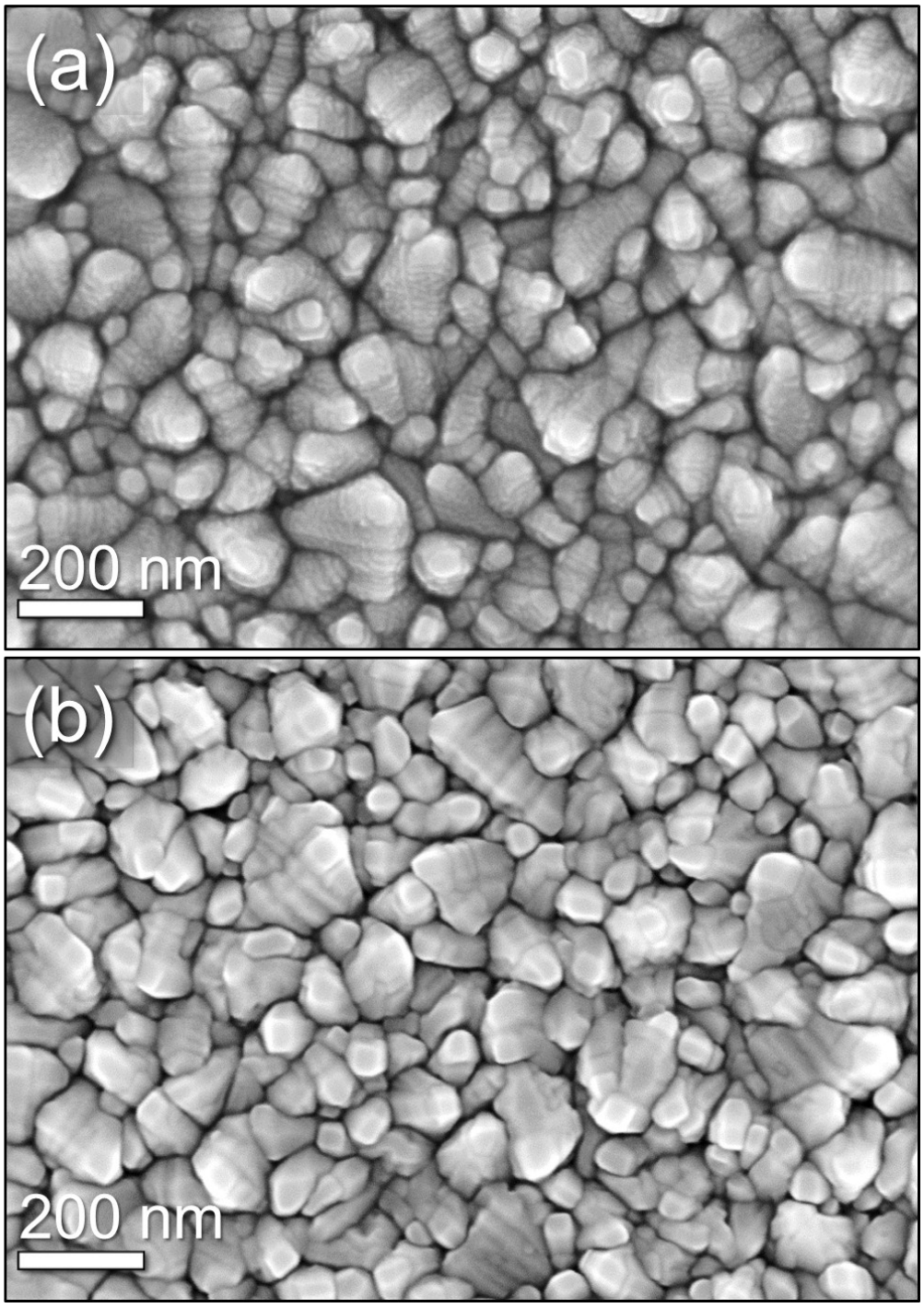

Figure S1. High magnification HRSEM images of (a) Si- and (b) Sn-doped hematite films.

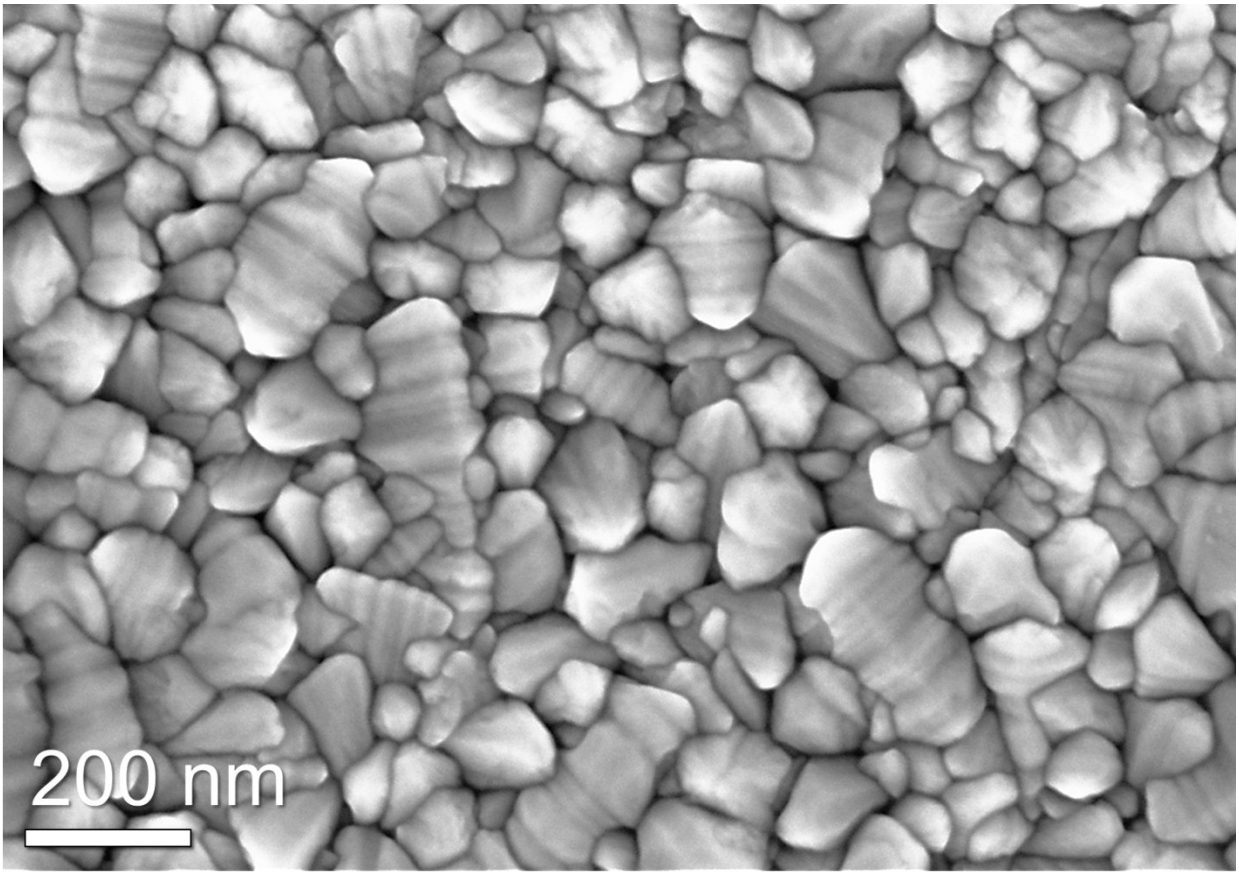

Figure S2. High magnification HRSEM image of pristine (uncoated) FTO surface.

Table S2. The Sherrer domain size in the doped hematite thin film photoanodes.

Dopant	Sherrer's domain size (nm)
Sn	10.9
Nb	12.6
Si	11.8
Pt	12.1
Zr	9.3
Ti	8.8
Zn	10.6
Ni	8.9
Mn	9.6

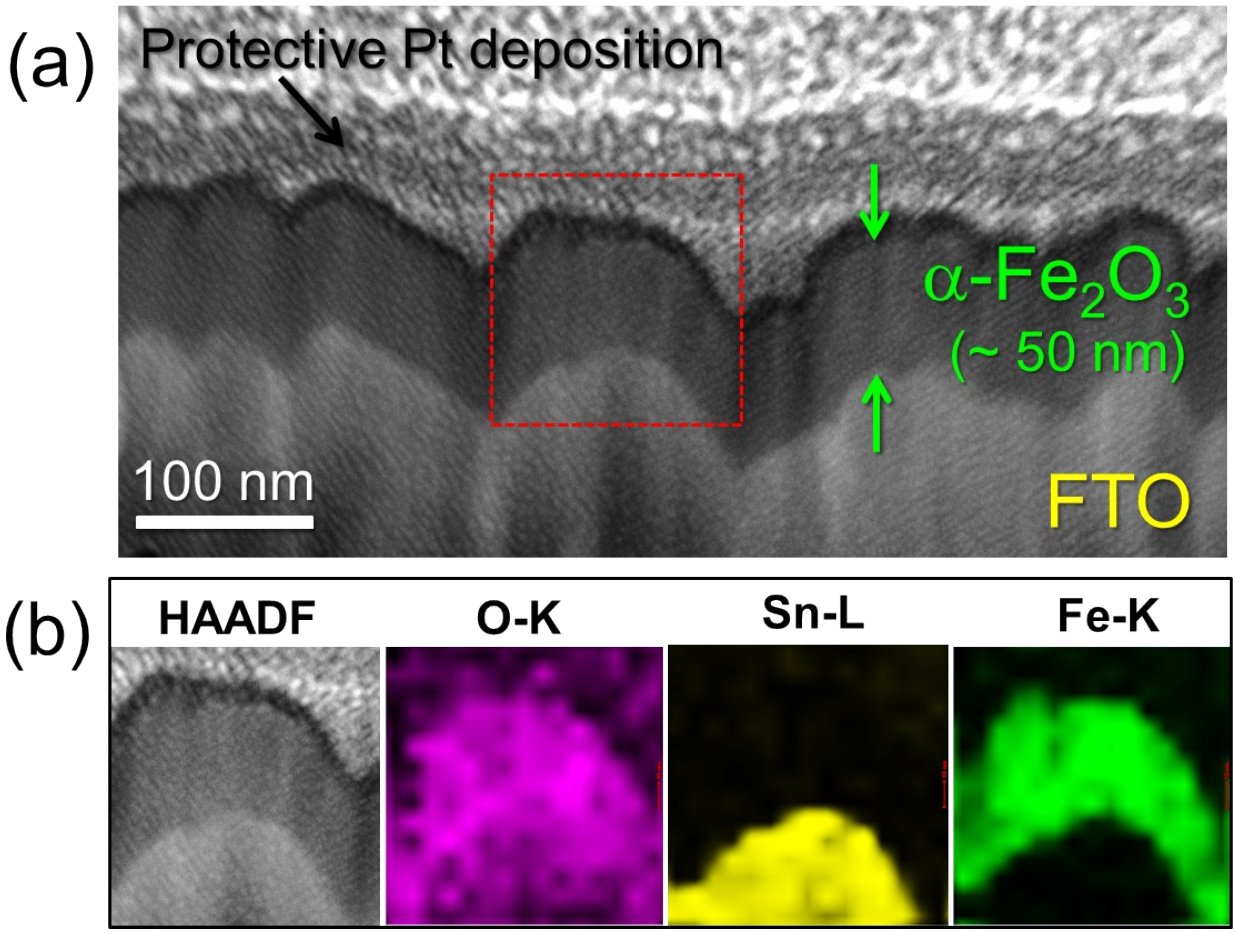

Figure S3. (a) Cross-sectional STEM-HAADF image of the Ti-doped hematite photoanode. (b) High magnification STEM-HAADF image and elemental maps of the O-K, Sn-L and Fe-K edge taken from the region shown by the red box in Figure (a).

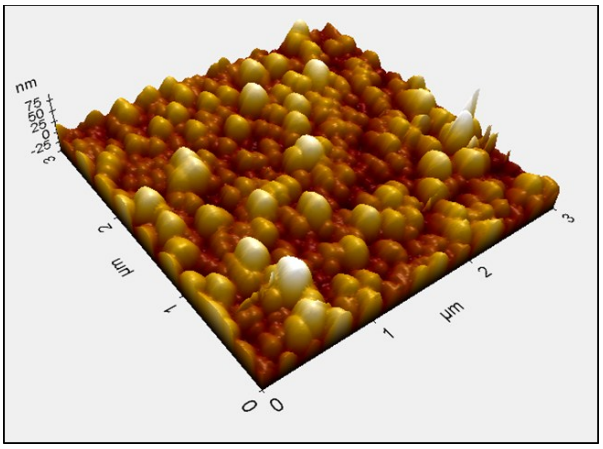

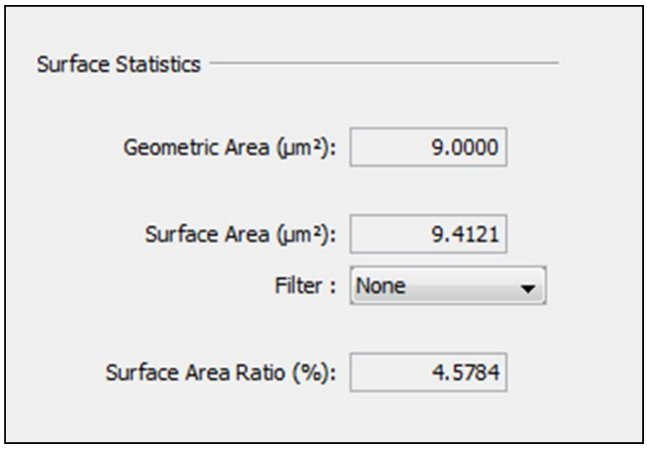

Figure S4. AFM image of the Ti-doped thin film hematite photoanode with measurement of the surface area enhancement due to roughness.

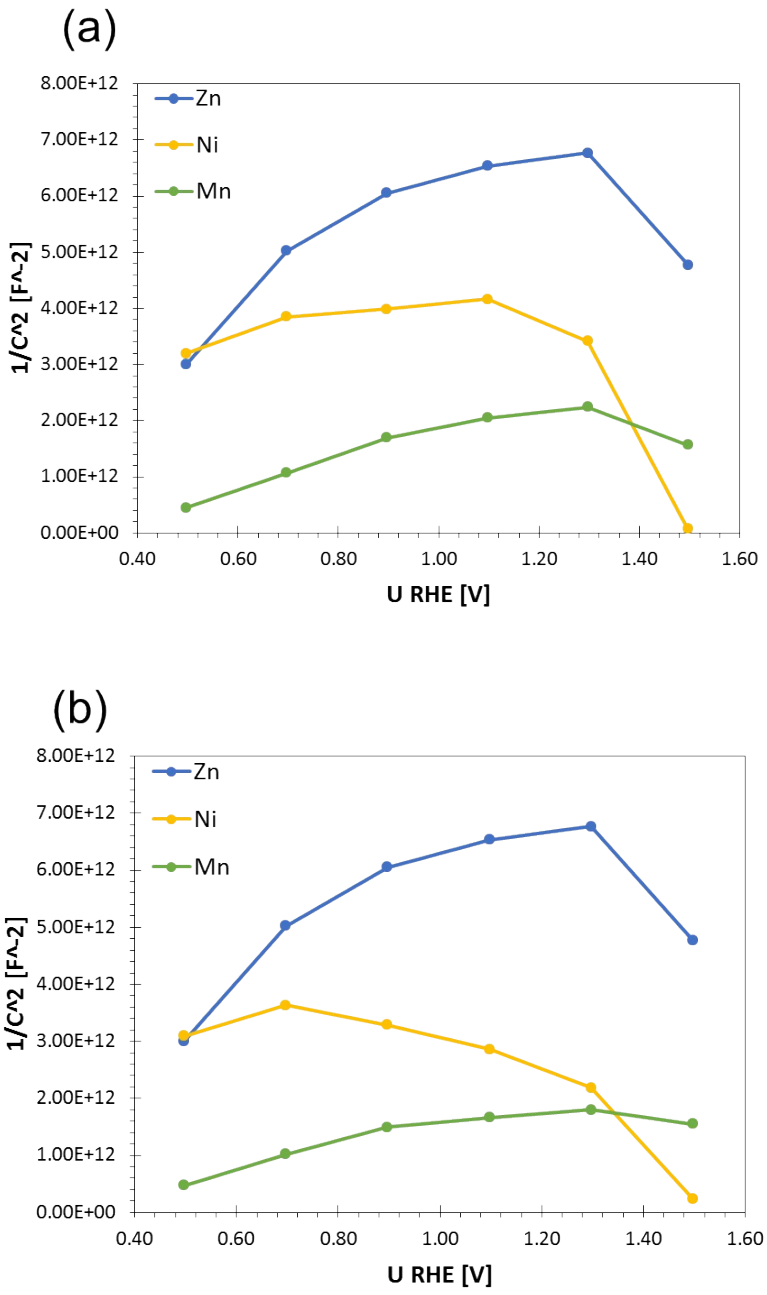

Figure S5. Mott-Schottky plots of Zn, Ni and Mn-doped hematite photoanodes at recorded at a frequency of 500 Hz in (a)1M NaOH with 0.5M H_2O_2 and (b) 1M NaOH.

Table S3. Selected frequencies (in Hz) for the Mott-Schottky analysis in (a) 1M NaOH and (b) 1M NaOH with 0.5M H_2O_2

(a) Dopants					
Ti	**Si**	**Pt**	**Zr**	**Sn**	**Nb**
25119	15849	19953	19953	19953	25119
19953	12589	15849	15849	15849	19953
15849	10000	12589	12589	12589	15849
12589	7943	10000	10000	10000	12589
10000	6310	7943	7943	7943	10000
7943	5012	6310	6310	6310	7943
6310	3981	5012	5012	5012	6310
5012	3162	3981	3981	3981	5012
3981	2512	3162	3162	3162	3981
3162	1995	2512	2512	2512	3162
2512	1585	1995	1995	1995	2512
1995	1259	1585	1585	1585	1995
1585	1000	1259	1259	1259	1585
1259	794	1000	1000	1000	1259
1000	631	794	794	794	1000
794	501	631	631	631	794
631	398	501	501	501	631
501	316				501
398					398
316					
251					
200					

(b) Dopants					
Ti	**Si**	**Pt**	**Zr**	**Sn**	**Nb**
19953	19953	10000	39811	25119	19953
15849	15849	7943	31623	19953	15849
12589	12589	6310	25119	15849	12589
10000	10000	5012	19953	12589	10000
7943	7943	3981	15849	10000	7943
6310	6310	3162	12589	7943	6310
5012	5012	2512	10000	6310	5012
3981	3981	1995	7943	5012	3981

3162	3162	1585	6310	3981	3162
2512	2512	1259	5012	3162	2512
1995	1995	1000	3981	2512	1995
1585	1585	794	3162	1995	1585
1259	1259	631	2512	1585	1259
1000	1000	501	1995	1259	1000
794	794	398	1585	1000	794
631	631		1259	794	631
501	501		1000	631	501
398	398		794	501	398
	316		631		316
			501		
			398		

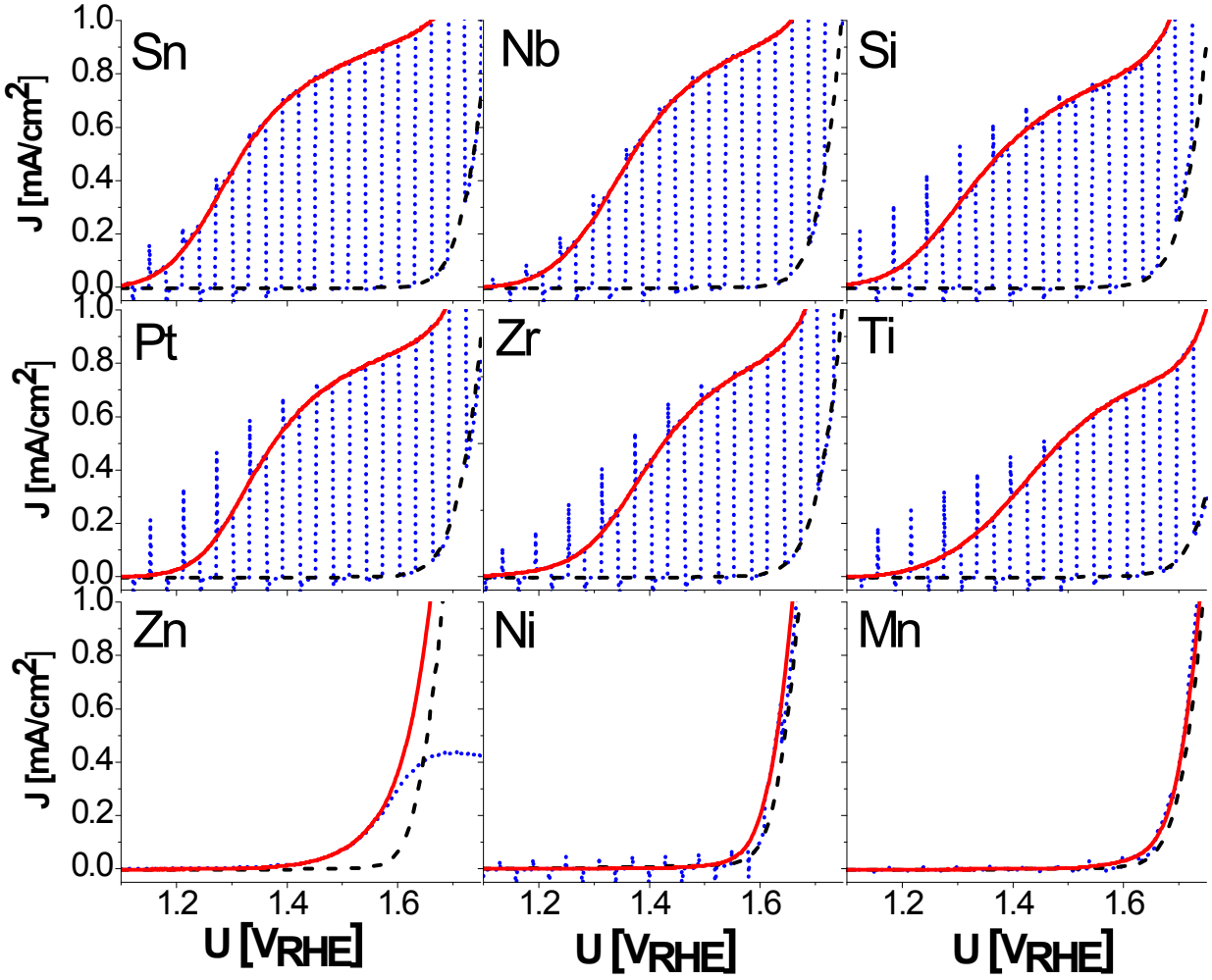

Figure S6. Dark (dashed lines), light (full lines) and chopped light (dash-dot lines) current vs. applied potential plots of thin film hematite photoanodes with different dopants measured in 1 M NaOH solution.

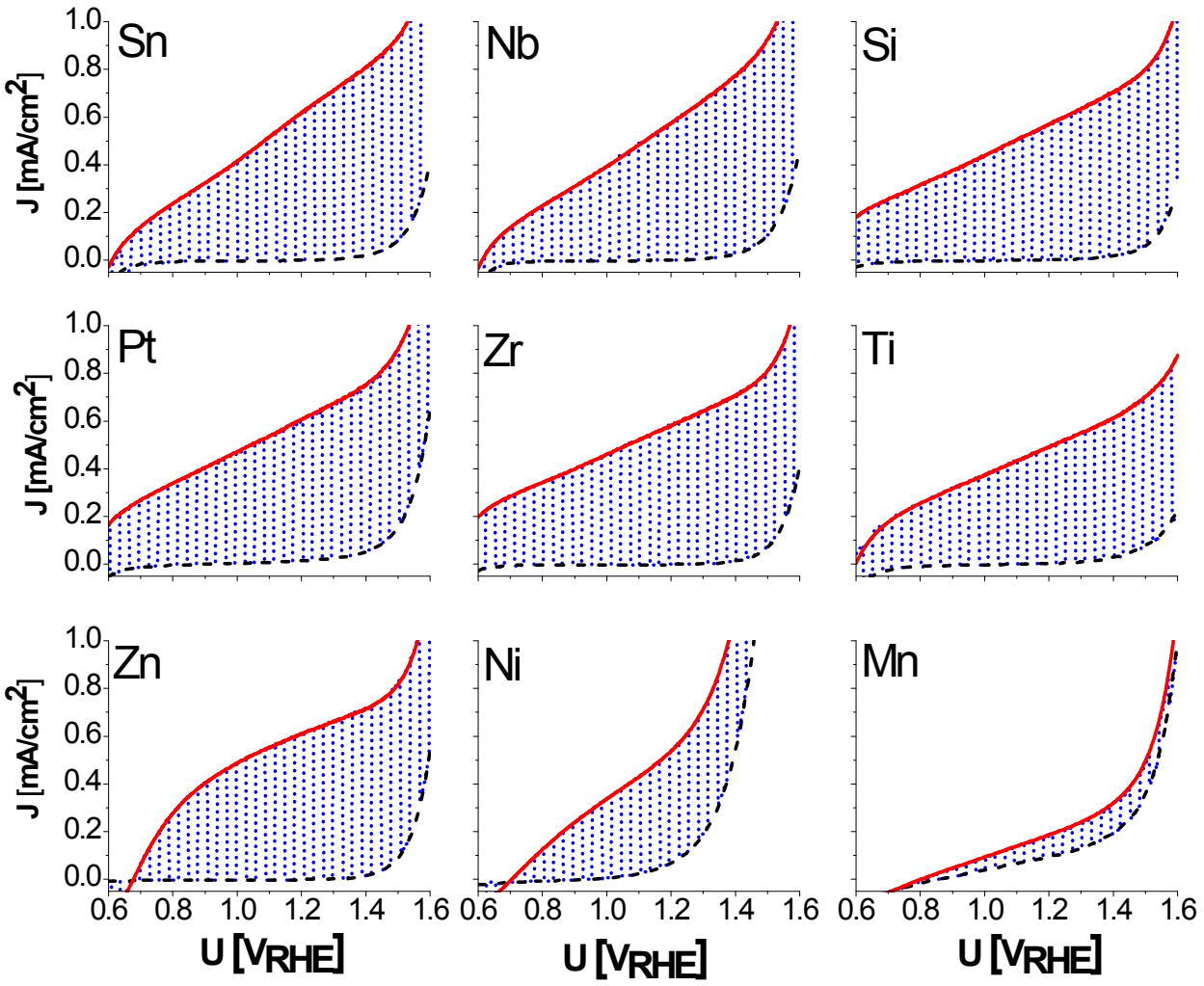

Figure S7. Dark (dashed lines), light (full lines) and chopped light (dash-dot lines) current vs. applied potential plots of thin film hematite photoanodes with different dopants measured in 1M NaOH + 0.5M H_2O_2 solution.

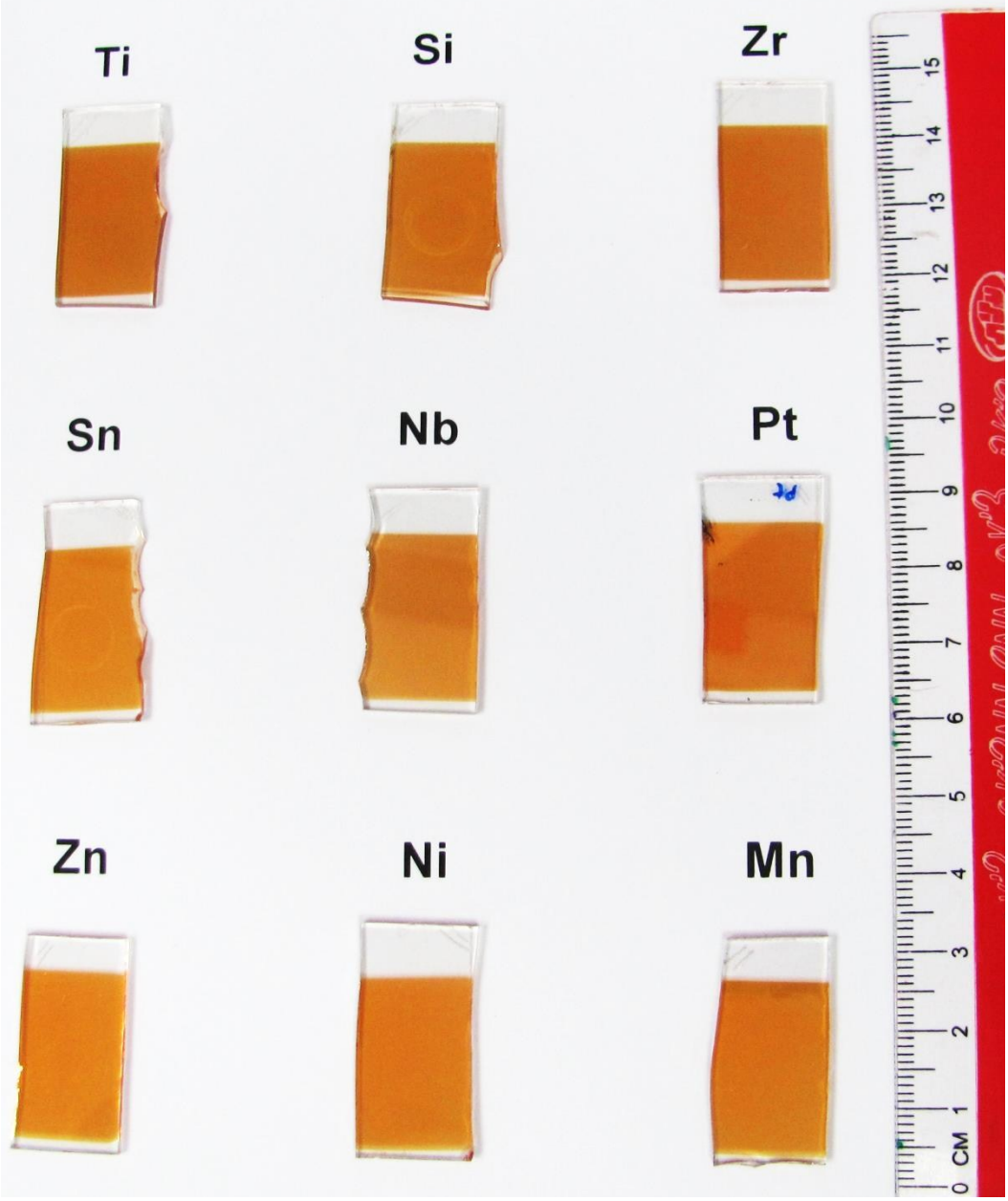

Figure S8. Photographs of the doped hematite photoanodes taken after the photoelectrochemical measurements.